

Electronic band structure of GaSe(0001): Angle-resolved photoemission and *ab initio* theory

L. Plucinski and R. L. Johnson

Institut für Experimentalphysik, Universität Hamburg, Luruper Chaussee 149, D-22761 Hamburg, Germany

B. J. Kowalski, K. Kopalko, and B. A. Orlowski

Institute of Physics, Polish Academy of Sciences, Al. Lotników 32/46, PL-02668 Warszawa, Poland

Z. D. Kovalyuk and G. V. Lashkarev

Institute for Problems of Materials Science, National Academy of Sciences of Ukraine, 3, Krzhizhanovsky st., Kiev-142, 03 680 Ukraine

(Received 9 May 2003; published 5 September 2003)

By performing extensive angle-resolved photoemission measurements using tunable linearly polarized synchrotron radiation with photon energies from 15 to 31 eV on high quality cleaved samples we have succeeded in experimentally mapping the occupied electronic bands of GaSe(0001) along all key symmetry directions. The experimental results are in very good agreement with state-of-the-art *ab initio* theoretical calculations. The data were analyzed assuming a direct transition model and final-state effects are discussed in the analysis of the normal-emission data. The off-normal emission spectra accurately reproduce the gaps in the calculated projected band structure. The azimuthal symmetry of the photocurrent revealed the polytype of the samples investigated.

DOI: 10.1103/PhysRevB.68.125304

PACS number(s): 73.90.+f, 71.15.Mb, 71.20.-b, 79.60.-i

I. INTRODUCTION

Recently there has been a revival in interest in III-VI semiconductors because they have remarkable nonlinear optical properties and when doped with transition metal ions form a new class of layered diluted magnetic semiconductors. Magnetic measurements on GaSe doped with Mn or Fe reveal remarkable differences in the magnetic interactions and anisotropy of these materials.¹ Gallium selenide is particularly interesting because it is transparent over the region from 0.65 to 18 μm with a very small absorption coefficient.² Thin films of gallium selenide have been grown on various substrates including Si(111) and GaAs(001).³⁻¹⁰

GaSe is a layered III-VI semiconductor, its crystal structure is highly anisotropic and consists of covalently bonded stacks of four atomic layers that are held together by a weak interstack interaction of the van der Waals type. The stack is a *sandwich* with top and bottom layers of Se and two layers of Ga ions in the middle (Se-Ga-Ga-Se). This essentially two-dimensional layered structure accounts for the very anisotropic mechanical properties. It was predicted from theoretical calculations¹¹⁻¹⁵ and confirmed by experimental band structure studies¹⁶⁻¹⁹ that in addition to the electronic states with two-dimensional properties there are also states with three-dimensional character. The unusual electronic properties of these layered semiconductors make them interesting both for theoretical investigations and potential applications.

II. EXPERIMENTAL

The samples were grown by an improved Bridgman-Stockbarger method in quartz ampoules at the Chernivtsi Division of the Institute for Problems of Materials Science, National Academy of Sciences of the Ukraine. Prior to the photoemission experiments clean surfaces were prepared by cleaving under ultrahigh vacuum (UHV) conditions. The natural cleavage plane is between the Se layers of the adja-

cent sandwiches and the surface normal is perpendicular to the sandwich layers. The samples were oriented *in situ* using low-energy electron diffraction (LEED). The angle-resolved photoemission experiments were performed in the 15–31 eV photon energy range at the F2.2 beamline at HASYLAB, Hamburg (Germany). This beamline is equipped with a Seya-Namioka monochromator and a VG ADES400 photoelectron spectrometer. The spherical sector electron energy analyzer is mounted on a goniometer that can be rotated in both azimuthal φ and polar ϑ angles around the sample. The measurements were performed with linearly polarized light incident at 45° in the *p* configuration.²¹ The electron energy analyzer was adjusted to lie on the plane defined by the incoming photons and the normal to the sample surface. The energy distribution curves (EDC's) were recorded with a typical resolution of 200 meV.

III. THEORETICAL CALCULATIONS

There are several GaSe polytypes which differ in the stacking sequence of the basis layer units;²² the three most important, β -GaSe, ε -GaSe, and γ -GaSe, are shown in Fig. 1 and the corresponding Brillouin zones are given in Fig. 2. The β and ε polytypes have a $2H$ stacking sequence (unit cell extends over two sandwiches with hexagonal symmetry) and the γ polytype has a $3R$ stacking sequence (three sandwiches, rhombohedral). Polytypes β and ε have eight atoms in the primitive cell (four Ga and four Se) and the γ polytype has four atoms in the primitive cell¹⁴ (two Ga and two Se). The band structures of the β and ε polytypes are very similar but that of the γ polytype is markedly different because it has four atoms in the primitive cell and correspondingly fewer valence bands in the reduced Brillouin zone. In this paper we will concentrate on the ε and γ polytypes.

The density functional theory (DFT) calculations were performed within the local density approximation using the FHI98MD package.²³ Gallium and selenium atoms were rep-

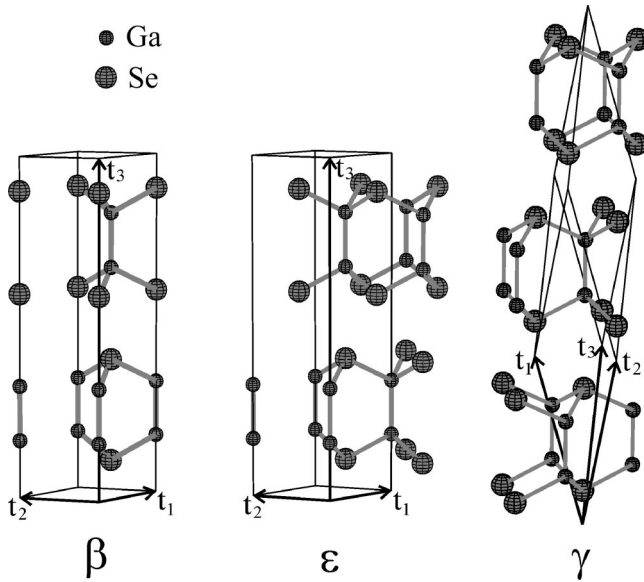


FIG. 1. Unit (primitive) cells for β -GaSe (left), ϵ -GaSe (middle), and γ -GaSe (right).

resented by norm-conserving scalar-relativistic pseudopotentials²⁴ Ga^{3+} and Se^{6+} (no Ga 3d levels were included in the Ga pseudopotential). An overview of the geometrical parameters is given in Table I. The experimental lattice constants depend on the polytype²⁵ and x-ray diffraction measurements on our GaSe samples²⁶ gave an experimental lattice constant $c = 16.0 \text{ \AA}$ for the dominating polytype. For consistency we decided to use the lattice constants given in Ref. 13 for our theoretical calculations.²⁷ The atomic positions in the plane perpendicular to the c axis are close-packed hexagonal and depend only on the lattice constant a ; the distance between the adjacent sandwiches depends on the lattice constant c . An overview of the structures and atomic coordinates of the different polytypes is given in Refs. 14 and 25. The intrasandwich distances between the inner Ga layers and outer Se layers along the c axis are particularly important and have a big impact on the band dispersions as discussed in the literature.¹² The calculations presented in this paper were performed with these parameters

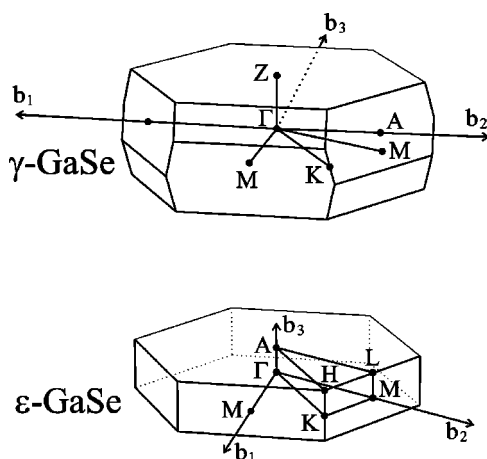


FIG. 2. Brillouin zones for γ and ϵ -GaSe polytypes.

fixed as in Ref. 13 for the case of the β polytype. The influence of the intrasandwich distances on the DFT-LDA band dispersions will be discussed elsewhere.²⁸ It is well known that the DFT-LDA approach cannot describe van der Waals interactions adequately^{29,30} and our attempt to determine the structure via energy optimization using the DFT code did not produce the desired result.³¹

The bulk band structure of ϵ -GaSe along selected high symmetry directions in the Brillouin zone is presented in Fig. 3 where the zero of the energy scale was adjusted to the valence band maximum (VBM). In this work we concentrate on the subbands indicated by I, II, and III in Fig. 3 which originate from the hybridization of Se 4p with Ga 4s and 4p orbitals.¹¹ The lowest band appearing at Γ between -14.41 and -14.04 eV derives from Ga 4s orbitals. As is usual for the LDA approximation the calculations for ϵ -GaSe yield a small direct fundamental gap at Γ of only 0.267 eV whereas experimentally it has an indirect gap of 2.065 eV.²⁰ In Fig. 3 the conduction bands were shifted to fit the experimental direct gap at Γ of 2.120 eV.²⁰ The density-of-states (DOS) shown in Fig. 3 was calculated using 720 k points in the irreducible Brillouin zone with a small Gaussian broadening of 0.10 eV, however, the DOS calculated with 420 k points already was qualitatively very similar.

Comparing our band structure to the one recently presented by Camara *et al.*¹¹ on the β polytype (β and ϵ polytypes have nearly identical band structures—our DFT-LDA calculations, for example, revealed differences less than 0.01 eV in the Γ -A direction) we find significant differences in the energies of several bands. Camara *et al.* reported -6.8 eV for the bottom of the subband III at M whereas our calculation gives -7.73 eV. At Γ subband II appears in our calculation between -4.96 and -3.86 eV which is nearly 1 eV higher than in the calculation of Camara *et al.* The width of the subband I of 1.78 eV at Γ is significantly larger in our calculation. Nevertheless the overall shape of the valence bands is similar in both calculations and differ qualitatively from the earlier results given in Refs. 12–14.

In Fig. 3 the gray-shaded areas show the bulk band structure projected on the (0001) surface for the $\Gamma ML A$ and $\Gamma KMLHA$ planes sampled with 10 k points in k_{\perp} . The overlap of the bands along Γ -K-M and A-H-L and the small dispersion reveals the two-dimensional nature of the bands.

TABLE I. Primitive vectors, intrasandwich distances and lattice constants used in our calculations.

| ϵ -GaSe | γ -GaSe |
|---|--|
| $\mathbf{t}_1 = (-a, 0, 0)$ | $\mathbf{t}_1 = (-a/2, -a/(2\sqrt{3}), c/2)$ |
| $\mathbf{t}_2 = (-a/2, a\sqrt{3}/2, 0)$ | $\mathbf{t}_2 = (a/2, -a/(2\sqrt{3}), c/2)$ |
| $\mathbf{t}_3 = (0, 0, c)$ | $\mathbf{t}_3 = (0, a/\sqrt{3}, c/2)$ |
| Intrasandwich distances | |
| $D_{\text{Ga-Ga}} = 0.154 \times c$ | $D_{\text{Se-Se}} = 0.300 \times c$ |
| Lattice constants (\AA) | |
| $a = 3.755$ | $c = 15.94$ |

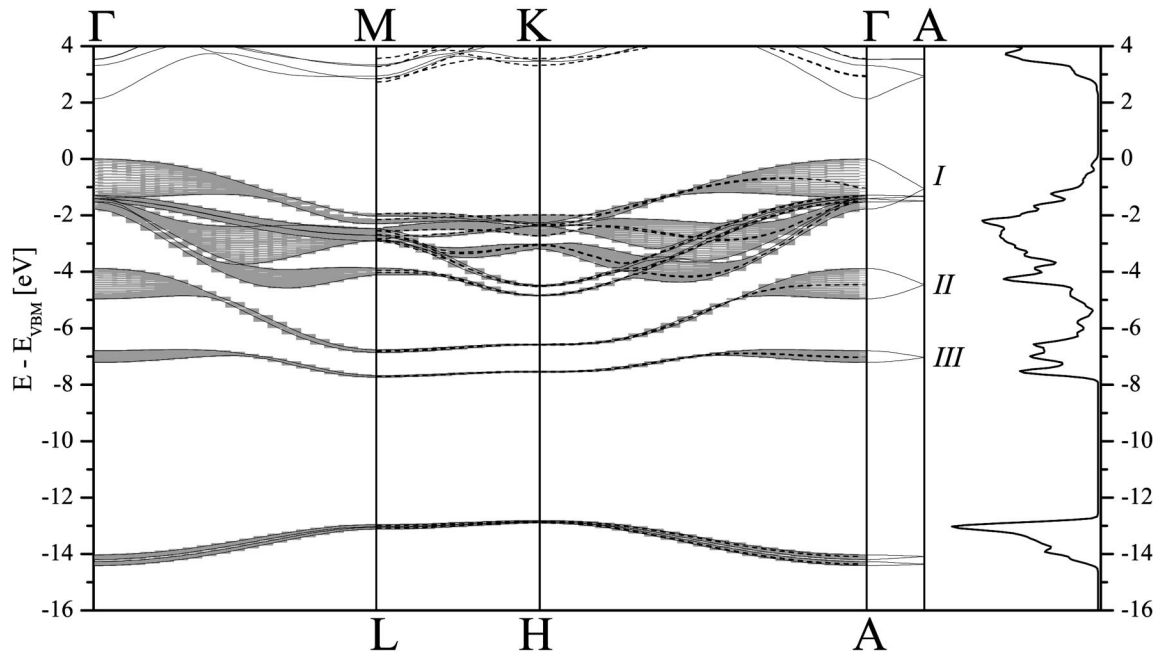


FIG. 3. Theoretical bulk band structure of ϵ -GaSe. Solid lines show the bands along Γ - M - K - Γ - A as indicated at the top of the figure. Dashed lines show bands along L - H - A as indicated at the bottom of the plot. Shaded areas show the occupied projected bulk band structure for the Γ MLA and Γ $KMLHA$ planes. The zero of the energy scale set to the VBM, and the direct gap at Γ was adjusted to 2.120 eV as given in Ref. 20. The density-of-states is shown on the right hand side.

It is clear that subbands II and III are two dimensional within the experimental accuracy over a significant portion of the Brillouin zone particularly in the $KMLH$ rectangle. This holds for the bottom of subband I, however, in subband I the projections of some bands have significant widths.

Figure 4 shows subband I for both ϵ and γ polytypes. The energetic positions of the bands are very similar for the two polytypes and in k_{\perp} direction the differences are not larger than 0.01 eV, but in γ -GaSe half of the bands are missing because it has half the number of atoms in the primitive cell. The expanded energy scale in Fig. 4 allows the bands to be distinguished and the dispersive structure I (a) can be readily separated from the relatively flat I (b) bands.

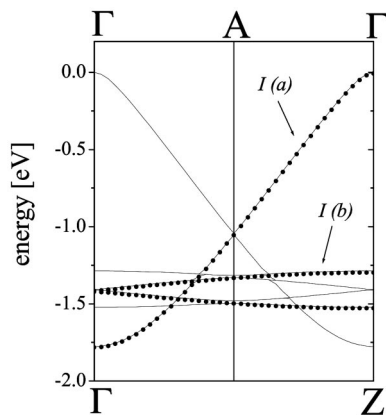


FIG. 4. Band structure of subband I along Γ - A - Γ for ϵ -GaSe (solid lines) and Γ - Z for γ -GaSe (dots).

IV. EXPERIMENTAL RESULTS

A. Azimuthal scans

Larsen *et al.*³² showed that an InSe sample could be oriented by measuring azimuthal scans of the photocurrent by rotating the sample about its surface normal. Here we present similar results on GaSe although our samples were initially oriented using LEED; both methods gave the same orientation. The azimuthal scan is performed by rotating the sample keeping the position of the electron analyzer fixed ($40^{\circ} < \vartheta < 60^{\circ}$). A detailed analysis of such scans on layered tantalum dichalcogenides, was performed by Smith and Traum³³ and the azimuthal dependence was found to have either a threefold or a sixfold symmetry. The Fermi surface measurements on $TiTe_2$ performed by Rossnagel *et al.*³⁴ employed azimuthal scans at the Fermi edge.

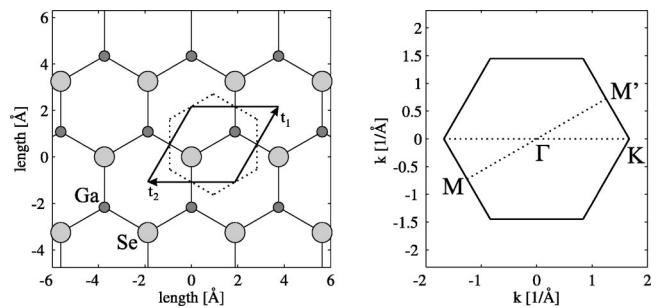


FIG. 5. Left: top view of the GaSe(0001) surface. The primitive hexagonal cell is indicated by dotted lines and the primitive cell used in the band structure calculations of ϵ and β -GaSe by a solid line. Right: the corresponding Brillouin zone with M and M' points indicated.

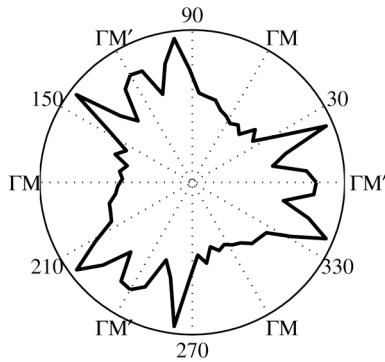


FIG. 6. Azimuthal scan of the Ga 3d level taken at $\vartheta=60^\circ$ with a photon energy $h\nu=39$ eV.

Figure 5 shows a top view of the GaSe(0001) surface which can also be regarded as a projection of one sandwich on the surface plane. The GaSe(0001) surface has threefold rotational symmetry and so the Γ - M and Γ - M' directions are nonequivalent. By employing the bond between the second layer Ga and the surface Se as a reference (e.g., within the unit cell in Fig. 5) we define that the Γ - M direction points from Ga to Se and Γ - M' from Se to Ga. Using the primitive vectors \mathbf{t}_1 and \mathbf{t}_2 as defined in Fig. 5 the vector $-\mathbf{t}_1 + \mathbf{t}_2$ is along Γ - M and $\mathbf{t}_1 - \mathbf{t}_2$ along Γ - M' .

As a test to unambiguously distinguish between the Γ - M and Γ - M' directions we have performed an azimuthal scan of the Ga 3d level. This scan was performed with a resolution of 500 meV and an energy window of ± 0.25 eV was taken to evaluate the intensity of the Ga 3d levels. The result shown in Fig. 6 reveals the threefold symmetry of the photocurrent. In the experiments we could only scan 120° of azimuthal dependence due to limitations of our UHV manipulator so the data were extrapolated to produce the figure. There are several reasons why the observed symmetry is not hexagonal, however, screening effects in the final state as discussed in Ref. 33 seem to be the most plausible explanation.³⁵ Since the 3d levels are localized on Ga atoms the final state screening is larger in the Γ - M direction and a higher photocurrent is expected in the Γ - M' direction.

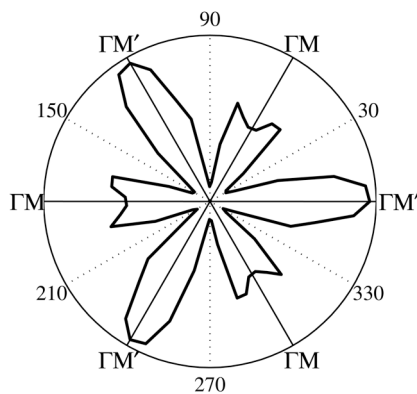


FIG. 7. Azimuthal scan of the valence band feature at $E_i=-1.55$ eV with respect to the VBM recorded for $\vartheta=40^\circ$.

Additional structure in the azimuthal intensity may be related to emission from Ga atoms in the lower layer of the sandwich.

The azimuthal scans in Figs. 7 and 8 were recorded by fixing the initial energy with respect to the VBM at -1.55 and -6.85 eV, respectively, and integrated over energy windows ± 0.15 eV while turning the sample around its normal. The resolution of the analyzer was set to 150 meV. These initial energies correspond to the top of band I and to band II and both result from the hybridization of the Se 4p with Ga 4s valence orbitals with a dominant Se contribution. A larger Ga 4s contribution is expected for the feature related to sub-band II according to the partial DOS calculated by Camara *et al.*¹¹ As in the case of the Ga 3d scan the azimuthal dependencies of the photocurrent presented in Figs. 7 and 8 have threefold symmetry.

The intensities of the spectral features should depend mainly on the structure of a single sandwich and not on the multilayer stacking sequence. In the ϵ and γ -GaSe polytypes there are only primitive translations between adjacent sandwiches and no rotations. The $(\bar{1}100)$ surface of GaSe can be regarded as polar for the ϵ and γ polytypes and non-polar for the β polytype. Only if the sample were ideally terminated and step-free would the β -polytype have threefold symmetry. Since the illuminated sample area at our beamline is macroscopic ($\sim 1 \times 4$ mm²) the threefold symmetry of the photocurrent is only to be expected from ϵ and γ -GaSe. These results clearly indicate that our samples were either of polytype ϵ , or γ , or a mixture of the two. MBE grown samples prepared by Koebel *et al.*⁵ and Dai *et al.*⁴ were γ polytype, however, for single crystals typically a mixture of ϵ and γ is reported.²⁵ In our experiments different cleaves on the same sample gave the same orientation from the photocurrent indicating long-range three-dimensional ordering.

B. Normal emission

Previous angle-resolved photoemission experiments with synchrotron radiation on GaSe (Ref. 17) assumed that the electronic structure was essentially two-dimensional and did

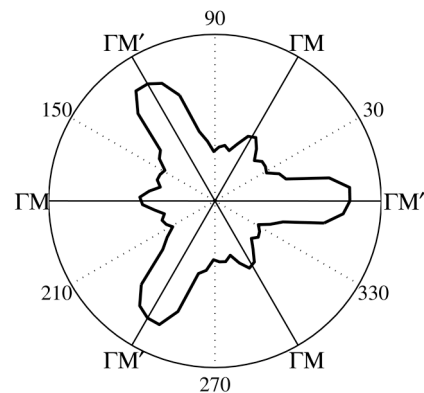


FIG. 8. Azimuthal scan with the same parameters as in Fig. 7 but for the lower peak in the valence band at $E_i=-6.85$ with respect to the VBM.

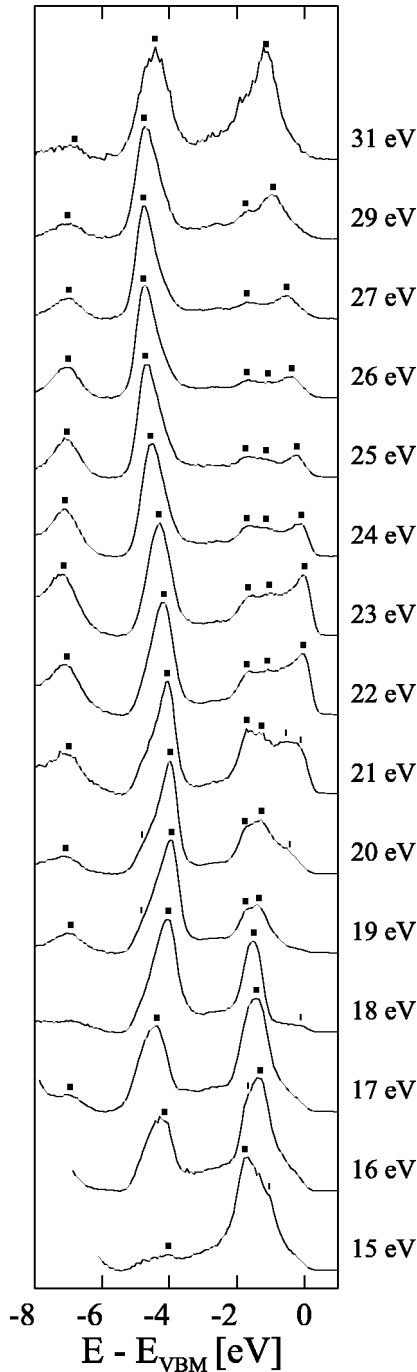


FIG. 9. Set of normal emission EDC's from GaSe. Thicker ticks indicate clearly dispersive peaks and thinner ticks less well-defined spectral features. The zero of the energy scale was set to the VBM.

not attempt to map the band dispersions along the Γ -A [0001] direction. However, the theoretical calculations predict significant dispersion along Γ -A. Here we will show that the experimental dispersions obtained from normal-emission measurements within a simple free-electron final state model are in good agreement with our calculated DFT-LDA band structure. The comparison of the DFT-LDA final bands with free-electron final states provides insight into the surprisingly good agreement between theory and experiment.

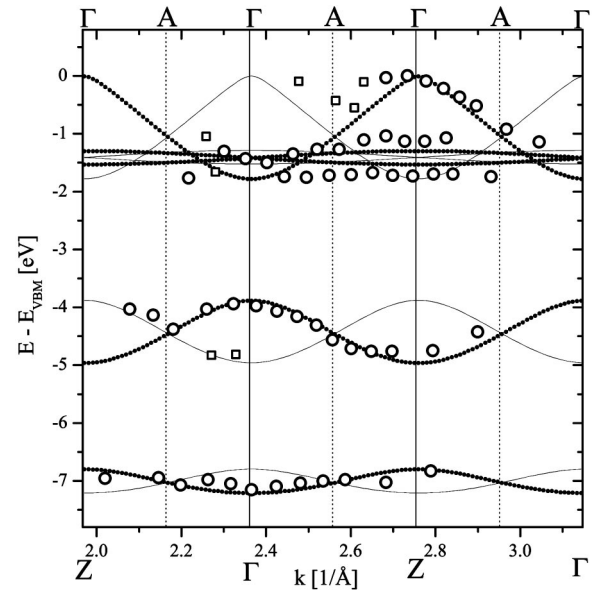


FIG. 10. Band structure constructed out of the features indicated in Fig. 9. Circles represent features clearly visible in the EDC's and the squares other features. Solid lines show the theoretical result for ϵ -GaSe along Γ -A as indicated on the top of the plot. The dotted lines show the theoretical results for γ -GaSe along Γ -Z as indicated at the bottom of the plot.

Figure 9 shows a set of normal-emission spectra measured for photon energies between $h\nu=15$ and 31 eV. The spectra contain several well-defined features with the most pronounced at around -4.5 eV (with respect to the VBM). The energy positions of the features were found with the help of inverted second derivatives and are indicated in Fig. 9 by ticks. The emission at the VBM is clearly seen as a shoulder in the spectra at around $h\nu=23$ eV. The features indicated in Fig. 9 were used to construct the band structure shown in Fig. 10 which also includes the theoretical bands. Wave vectors \mathbf{k} were calculated assuming free-electron final states using

$$k_{\perp} = \sqrt{\frac{2m}{\hbar^2}(E_{\text{kin}} + V_0)}, \quad (1)$$

where E_{kin} is the kinetic energy of the electrons and V_0 is the *inner potential* representing the potential barrier at the surface in this model. Typically V_0 is fitted to provide best agreement with the theoretical calculations and for Fig. 10 $V_0=10$ eV was used.

The agreement between theory and experiment is very good for subband II. The feature related to the subband II is clearly visible in our spectra and provides an unambiguous comparison with theory. The energetic position of the less dispersive subband III is reproduced well in our data. This indicates that our theoretical value for the bottom of this band of -7.16 eV at Γ is a better estimate than the values from earlier calculations.¹¹⁻¹⁵

The agreement for the subband I is good, but there are some discrepancies. There are several weaker features in this region which do not fit the theoretical calculation, however,

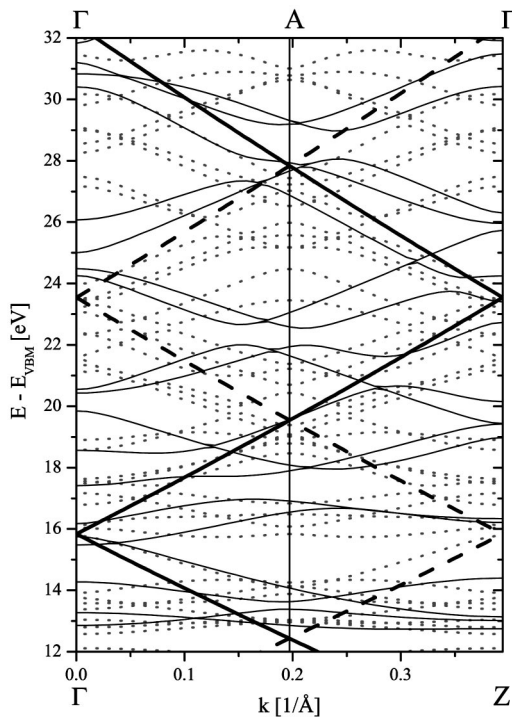


FIG. 11. DFT-LDA final bands for ϵ (dotted line) and γ -GaSe (thinner solid line) with free-electron (primary-cone) final bands for ϵ (dashed line) and γ -GaSe (thicker solid line). Free-electron bands for ϵ -GaSe lie on the γ -GaSe lines.

the width of subband I compares very well with our prediction. The calculation gives the top of the subband I(b) to be -1.287 eV whereas experimentally it is found at -1.1 eV, however, our theoretical analysis indicates that the position of the subband I(b) can be varied by regulating the intrasandwich lattice distance.

In Fig. 10 it can be seen that the experimental data points lie on the bands shared by ϵ and γ polytypes. At first glance it would appear that our samples were mainly γ polytype, however, the contributions from ϵ -GaSe could be masked due to the symmetry selection rules in photoemission. It is worth noting that one of the challenges in the analysis of the normal emission data from GaSe was to cope with the relatively short distance between Γ and A in the Brillouin zone of ϵ -GaSe since the features indicated in Fig. 9 lie away from the first ϵ -GaSe Brillouin zone.

The additional small features in the energy region between -2 and -4 eV in the EDC's in Fig. 9 may be due to the coupling of bulk and surface imperfections to the high DOS. They were not included in the experimental band structure because of their low intensity and because for such features a direct transition model would be inappropriate. We could not identify any special surface-related features.

A central problem in analyzing angle-resolved photoemission data is the choice of appropriate final bands (FB's) to calculate the initial \mathbf{k} vectors. Typically for energies greater than 25 eV the complex array of calculated FB's behaves effectively as a parabolic band for generating the photoemission spectra. At lower energies there are typically distinct

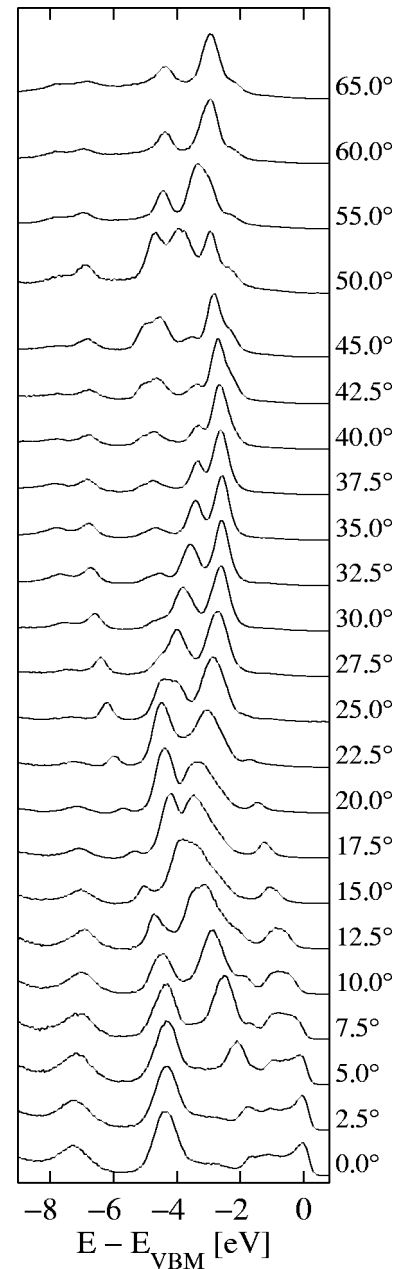


FIG. 12. Set of off-normal spectra at constant $h\nu = 23$ eV for $\Gamma KMLHA$ emission plane. The zero of the energy scale was set to the VBM.

features in EDC's which cannot be explained within the free-electron final-state model. In general it is possible to establish the FB's using *ab initio* calculations together with inverse photoelectron spectroscopy, or very-low-energy electron diffraction.³⁶ Here we compare the DFT-LDA FB's with free-electron final states. The results for the final energy range 12–32 eV are shown in Fig. 11, where the final bands were shifted to fit the experimental direct band gap of 2.120 eV at Γ . Such shifting of the LDA final states has been shown to be justified for II-VI compounds from GW calculations³⁷ for final state energies up to 35 eV, however, it is not guaranteed to work well for layered III-VI compounds. Figure 11 shows that for both γ -GaSe and ϵ -GaSe there are

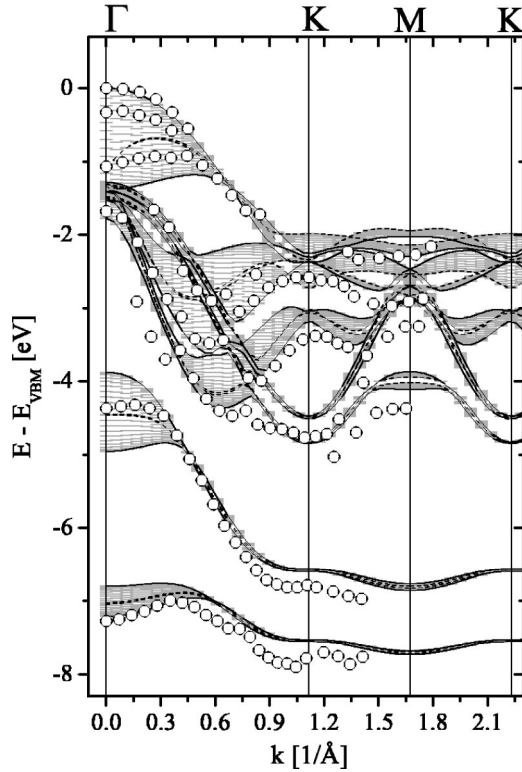


FIG. 13. Band structure for the $\Gamma KMLHA$ emission plane. Solid lines show the calculated band structure along Γ - K - M , the dashed line along A - H - L and the gray areas show the projected band structure.

final state bands which lie in the vicinity of the free-electron parabola and this explains the unexpectedly good agreement found in Fig. 10.

C. Off-normal emission

The normal-emission photoemission results clearly reveal the three-dimensional character of the GaSe band structure. Here we present off-normal spectra collected for the $\Gamma KMLHA$ and ΓMLA emission planes and compare the results with the theoretical calculations.

Figure 12 shows a set of off-normal ARPES spectra for the $\Gamma KMLHA$ emission plane at a photon energy $h\nu = 23$ eV. This photon energy was chosen to be close to the Γ point for features near the VBM at small angles. Spectra were fitted with Gaussians and the \mathbf{k} vectors in the parallel direction were found using the formula

$$\mathbf{k}_{\parallel} = \sqrt{\frac{2m}{\hbar^2} E_k} \sin(\vartheta). \quad (2)$$

The corresponding band structure is shown in Fig. 13. Here we find comprehensive agreement between the experimental data and the theoretical results for all significant features appearing in the experimental spectra. All the experimental energy positions given in this section have an accuracy of ± 0.1 eV due to instrumental resolution and fitting precision. As in the normal-emission spectra the subbands II and III are

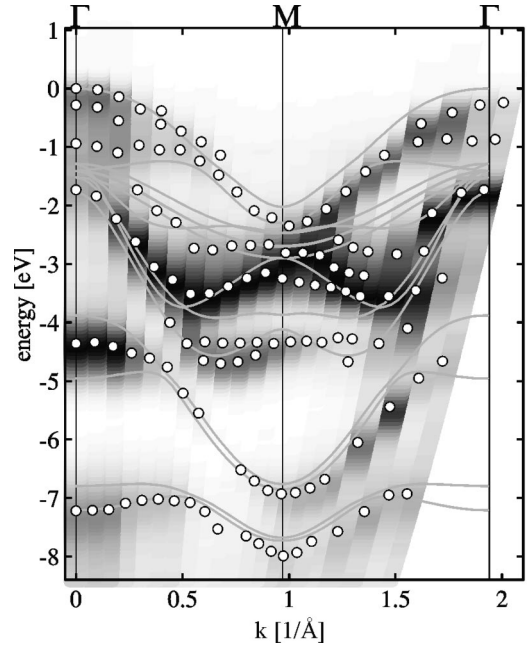


FIG. 14. Band structure for ΓMLA plane. In the background the off-normal spectra for $h\nu = 23$ eV are depicted as a gray-scale structure plot. The symbols represent the fitted spectral features and the solid lines the theoretical bands along Γ - M for ε -GaSe.

clearly reproduced, however, the experimental values are slightly lower at K lying at -6.8 eV for band II and -7.8 eV for band III. The experimental position of band I is slightly lower, however, the gaps in our projected band structure are compatible with experiment. The biggest difference is found for the two bands having energies -4.5 and -4.8 eV at the K point. These significantly two-dimensional bands are a continuation of subband I(b) which becomes more dispersive in the “off-normal” direction. The upper subband is found at K and M with the experimental values -4.75 and -3.25 eV, respectively, and the lower subband at M is located at -4.35 eV.

In Fig. 14 the band structure for the ΓMLA emission plane is shown together with the experimental spectra plotted on a gray-scale using Eq. (2). At M the experimental energies of the subbands II and III are -6.9 and -8.0 eV, respectively, and the subbands I(b) are located at -3.30 and -4.35 in very good agreement to the results obtained for the $\Gamma KMLHA$ plane.

V. SUMMARY

Gallium selenide layered crystals have been studied by angle-resolved photoemission using linearly polarized synchrotron radiation with photon energies 15–31 eV. The three-fold symmetry of the photocurrent intensity in azimuthal scans allowed us to identify that the samples we measured were either ε , γ , or a mixture of the two polytypes. From the Ga $3d$ azimuthal scan we could distinguish unambiguously between the Γ - M and Γ - M' Brillouin zone directions. Normal emission results analyzed within the free-electron final-state model gave good agreement with *ab initio* theoretical

calculations performed with the intrasandwich distances given in Ref. 13. Comparison of the DFT-LDA and free-electron final states indicated why free-electron final states could be used to analyze the normal emission data. The off-normal data allowed us to determine the energies of several bands at the high symmetry points K and M with an accuracy of ± 0.1 eV. Finally, it should be noted that the results reported here on GaSe probably represent the best agreement between *ab initio* DFT theoretical calculations and experimental photoemission band-mapping achieved to date.

ACKNOWLEDGMENTS

We would like to thank the HASYLAB staff for their assistance and fruitful discussions with Andrzej Fleszar are acknowledged. L.P. would like to acknowledge the support of the DFG-Graduiertenkolleg 463 "Spektroskopie an Lokalisierten Atomaren Systemen." The work was supported by KBN (Poland) Projects No. 2 P03B 046 19, 2 P03B 020 17, SPUB-M/DESY/P-03/DZ-213/2000, BMBF Project No. 05 KSIGUC/3 and by the IHP Contract No. HPRI-CT-1999-00040 of the European Commission.

-
- ¹T.M. Pekarek, C.L. Fuller, J. Garner, B.C. Crooker, I. Miotkowski, and A.K. Ramdas, *J. Appl. Phys.* **89**, 7030 (2001).
- ²N.C. Fernelius, *Prog. Cryst. Growth Charact. Mater.* **28**, 275 (1994).
- ³S. Meng, B.R. Schroeder, and M.A. Olmstead, *Phys. Rev. B* **61**, 7215 (2000).
- ⁴Z.R. Dai, S.R. Chegwidan, L.E. Rumaner, and F.S. Ohuchi, *J. Appl. Phys.* **85**, 2603 (1999).
- ⁵A. Koëbel, Y. Zheng, J.F. Pétrouff, M. Eddrief, V.L. Thanh, and C. Sébenne, *J. Cryst. Growth* **154**, 269 (1995).
- ⁶H. Abe, K. Ueno, K. Saiki, and A. Koma, *Jpn. J. Appl. Phys.* **32**, L1444 (1993).
- ⁷J.E. Palmer, T. Saitoh, T. Yodo, and M. Tamura, *J. Appl. Phys.* **74**, 7211 (1993).
- ⁸V.L. Thanh, M. Eddrief, J.E. Mahan, A. Vantomme, J.H. Song, and M.-A. Nicolet, *J. Appl. Phys.* **81**, 7289 (1997).
- ⁹J.-Y. Emery, L. Brahim-Ostmane, C. Hirlimann, and A. Chevy, *J. Appl. Phys.* **71**, 3256 (1992).
- ¹⁰N. Kambe, *J. Appl. Phys.* **69**, 2697 (1991).
- ¹¹M.O.D. Camara, A. Mauger, and I. Devos, *Phys. Rev. B* **65**, 125206 (2002).
- ¹²M. Schlüter, J. Camassel, S. Kohn, J.P. Voitchovsky, Y.R. Shen, and M.L. Cohen, *Phys. Rev. B* **13**, 3534 (1976).
- ¹³E. Doni, R. Girlanda, V. Grasso, A. Balzarotti, and M. Piacentini, *Nuovo Cimento Soc. Ital. Fis., B* **51**, 154 (1979).
- ¹⁴S. Nagel, A. Baldereschi, and K. Maschke, *J. Phys. C* **12**, 1625 (1979).
- ¹⁵J.V. McCanny and R.B. Murray, *J. Phys. C* **10**, 1211 (1977).
- ¹⁶G. Margaritondo, J.E. Rowe, and S.B. Christman, *Phys. Rev. B* **15**, 3844 (1977).
- ¹⁷P. Thiry, Y. Petroff, R. Pinchaux, C. Guillot, Y. Ballu, J. Lecante, J. Paigné, and F. Levy, *Solid State Commun.* **22**, 685 (1977).
- ¹⁸F. Antonangeli, M. Piacentini, A. Balzarotti, V. Grasso, R. Girlanda, and E. Doni, *Nuovo Cimento Soc. Ital. Fis., B* **51**, 181 (1979).
- ¹⁹P.M. Williams, *Nuovo Cimento Soc. Ital. Fis., B* **38**, 216 (1977).
- ²⁰E. Aulich, J.L. Brebner, and E. Mooser, *Phys. Solid State* **31**, 129 (1969).
- ²¹In the p configuration the polarization vector lies in the plane defined by the incoming photons and the surface normal of the sample.
- ²²A. Kuhn, R. Chevalier, and A. Rimsky, *Acta Crystallogr., Sect. B: Struct. Crystallogr. Cryst. Chem.* **31**, 2841 (1975).
- ²³M. Bockstedte, A. Kley, J. Neugebauer, and M. Scheffler, *Comput. Phys. Commun.* **107**, 187 (1997).
- ²⁴M. Fuchs and M. Scheffler, *Comput. Phys. Commun.* **119**, 67 (1999).
- ²⁵A. Kuhn, A. Chevy, and R. Chevalier, *Phys. Status Solidi A* **31**, 469 (1975).
- ²⁶E. Dynowska and J. Pelka (private communication).
- ²⁷To our knowledge the intralayer structure of GaSe polytypes is not known in detail and the most recent publication is Ref. 25.
- ²⁸L. Plucinski and R. L. Johnson (unpublished).
- ²⁹Y. Andersson, D.C. Langreth, and B.I. Lundqvist, *Phys. Rev. Lett.* **76**, 102 (1996).
- ³⁰R.O. Jones and O. Gunnarsson, *Rev. Mod. Phys.* **61**, 689 (1989).
- ³¹Using the DFT code to minimize the total energy we determined the relaxed atomic positions. For ϵ -GaSe the intrasandwich distances were $D_{\text{Ga-Ga}}=0.144 \times c$ and $D_{\text{Se-Se}}=0.275 \times c$. The convergence of the relaxation run was very good, however, the band structure calculated with the relaxed geometry did not compare well to the experimental results. At Γ subbands I(a) and I(b) were separated; I(a) appeared between 0 and -1.34 eV and I(b) between -1.59 and -1.83 eV.
- ³²P.K. Larsen, S. Chiang, and N.V. Smith, *Phys. Rev. B* **15**, 3200 (1977).
- ³³N.V. Smith and M.M. Traum, *Phys. Rev. B* **11**, 2087 (1975).
- ³⁴K. Rosnagel, L. Kipp, M. Skibowski, C. Solterbeck, T. Strasser, W. Schattke, D. Voss, P. Krüger, A. Mazur, and J. Pollmann, *Phys. Rev. B* **63**, 125104 (2001).
- ³⁵See Fig. 16 in Ref. 33.
- ³⁶V.N. Strocov, H.I. Starnberg, P.O. Nilsson, H.E. Brauer, and L.J. Holleboom, *Phys. Rev. Lett.* **79**, 467 (1997).
- ³⁷A. Fleszar and W. Hanke, *Phys. Rev. B* **62**, 2466 (2000).